Science of the Total Environment 468–469 (2013) S71–S84

Contents lists available at ScienceDirect

Science of the Total Environment

journal homepage: www.elsevier.com/locate/scitotenv

Glacial lakes in the Indian Himalayas — From an area-wide glacial lake inventory to on-site and modeling based risk assessment of critical glacial lakes

Raphael Worni [a,b,*], Christian Huggel [a,c], Markus Stoffel [a,b]

[a] Institute for Environmental Sciences, University of Geneva, route de Drize 7, CH-1227 Carouge, Switzerland
[b] Institute of Geological Sciences, University of Bern, Baltzerstrasse 1+3, CH-3012 Bern, Switzerland
[c] Department of Geography, University of Zurich—Irchel, Winterthurerstrasse 190, CH-8057 Zurich, Switzerland

HIGHLIGHTS

► We present the first comprehensive glacier lake inventory for the Indian Himalayas.
► In total, 251 glacier lakes >1 ha were mapped and classified.
► For three *critical* glacier lakes a detailed risk assessment was carried out.
► Risk assessment is based on field work, remote sensing and dynamic modeling.

ARTICLE INFO

Article history:
Received 24 April 2012
Received in revised form 15 October 2012
Accepted 9 November 2012
Available online 4 December 2012

Keywords:
Glacial lake inventory
Indian Himalayas
Glacial lake outburst flood (GLOF)
Risk assessment
Scenario modeling
BASEMENT

ABSTRACT

Glacial lake hazards and glacial lake distributions are investigated in many glaciated regions of the world, but comparably little attention has been given to these topics in the Indian Himalayas. In this study we present a first area-wide glacial lake inventory, including a qualitative classification at 251 glacial lakes >0.01 km^2. Lakes were detected in the five states spanning the Indian Himalayas, and lake distribution pattern and lake characteristics were found to differ significantly between regions. Three glacial lakes, from different geographic and climatic regions within the Indian Himalayas were then selected for a detailed risk assessment. Lake outburst probability, potential outburst magnitudes and associated damage were evaluated on the basis of high-resolution satellite imagery, field assessments and through the use of a dynamic model. The glacial lakes analyzed in the states of Jammu and Kashmir and Himachal Pradesh were found to present moderate risks to downstream villages, whereas the lake in Sikkim severely threatens downstream locations. At the study site in Sikkim, a dam breach could trigger drainage of ca. 16×10^6 m^3 water and generate maximum lake discharge of nearly 7000 m^3 s$^-$. The identification of critical glacial lakes in the Indian Himalayas and the detailed risk assessments at three specific sites allow prioritizing further investigations and help in the definition of risk reduction actions.

1. Introduction

Glacier retreat is observed in most regions of the Hindu Kush Himalaya (HKH; Bolch et al., 2012), which has given rise to the formation of numerous new glacial lakes. Glacial lakes are an indirect indicator of glacier change (Gardelle et al., 2011) and unstable lakes can present hazards to downstream locations (Costa and Schuster, 1988). Sporadic glacial lake outbursts may drain as powerful floods (Mergili et al., 2011), and are therefore considered the most important glacier-related hazard in terms of direct damage potential (Osti and Egashira, 2009). Glacial lake outburst floods (GLOFs) have killed thousands of people in many parts of the world (Carey, 2005; Clague and Evans, 2000; Richardson and Reynolds, 2000a), and some of the largest events occurred in the Himalayas (Bhargava, 1995; Osti and Egashira, 2009; Tashi, 1994; Vuichard and Zimmermann, 1986). As a result, GLOF risks are receiving increased attention as a key climate change hazard (Malone, 2010), and awareness for glacial lake monitoring and hazard mitigation has increased recently.

Glacial lake inventories with a prioritization of detected lakes are important as they allow non-specialist local authorities to quickly identify lakes where more detailed and comprehensive studies should be directed (Allen et al., 2009). Glacial lakes have been mapped and analyzed in different regions of the HKH (Hewitt, 1982; Yamada and Sharma, 1993), yet the focus of past studies has been predominantly on Bhutan (Fujita et al., 2008; Komori, 2008; Pitman et al., 2012), Nepal (Bolch et al., 2008; Yamada and Sharma,

* Corresponding author at: Institute of Geological Sciences, University of Bern, Baltzerstrasse 1+3, CH-3012 Bern, Switzerland. Tel.: +41 31 631 52 79; fax: +41 31 631 48 43.
E-mail addresses: raphael.worni@dendrolab.ch (R. Worni), christian.huggel@geo.uzh.ch (C. Huggel), markus.stoffel@dendrolab.ch (M. Stoffel).

0048-9697/$ – see front matter © 2012 Elsevier B.V. All rights reserved.
http://dx.doi.org/10.1016/j.scitotenv.2012.11.043

1993), and Tibet (Wang et al., 2008). A transboundary assessment of glacial lake distribution and evolution in the HKH was carried out by Gardelle et al. (2011) and also covered some regions in India; and ICIMOD (2010) compiled an extensive glacial lake inventory over large regions of the HKH, including three states in India. However, we are not aware of any glacial lake inventory covering the entire Indian Himalayas, and realize that generally few studies on glacial lakes have been carried out in the Indian Himalayas so far (Babu-Govindha-Raj, 2010; Randhawa et al., 2005).

An accurate and objective classification of glacial lakes is challenging but essential to maintain credibility towards stakeholders and local populations. Not all existing glacial lakes are unstable and most lakes will not burst out catastrophically (Huggel et al., 2004). Lake outburst probability is a function of the susceptibility of a dam to fail and the potential of external trigger processes (Richardson and Reynolds, 2000a). The stability of a dam depends primarily on its geometry, internal structure, and material properties (Costa and Schuster, 1988; Fujita et al., 2009; Korup and Tweed, 2007). Dam stability can change over time, as for instance melting of stagnant ice within moraine dams can contribute to weakening of overall dam structure (Clague and Evans, 2000; Richardson and Reynolds, 2000b; Worni et al., 2012a). Different authors (Huggel et al., 2004; Lu et al., 1999; Wang et al., 2008) proposed key parameters such as the dam width-to-height ratio, top width of dam, distal dam flank steepness or freeboard for a qualitative lake stability assessment. Parameters of most likely dam breaching help to assess the outburst probability of a particular lake. However, even unstable glacial lakes normally need a trigger to induce dam failure: Dams fail when the material strength is exceeded by driving forces that comprise, among others, the weight of the impounded water mass, seepage forces, earthquakes and shear stresses from overtopping flow or displacement waves (Korup and Tweed, 2007; Massey et al., 2010). Overtopping flows can be caused by heavy rainfall or a sudden influx of water from upstream sources. Displacement waves are, in contrast, triggered by mass movements entering the lake, such as snow and ice avalanches, rockfalls, debris flows or landslides (Carey et al., 2012; Clague and Evans, 2000; Costa and Schuster, 1988; Huggel et al., 2004). To assess the probability for mass impacts into a lake, potential starting zones of mass movements must be identified, possible magnitudes estimated and corresponding run-out distances evaluated. Alean (1985), for instance, analyzed ice avalanches in the Swiss Alps with volumes between 0.2 and 5×10^6 m^3, and found angles of reach between 17° and 32°. Such dimensions are useful to delimit a reasonable range of potential ice avalanches which might trigger a GLOF. Similar empirical relations are available for other mass-movement processes and are summarized by Rickenmann (2005).

For lake dams that are found to be susceptible to failure, magnitudes of potential GLOFs can be approximated with empirical relationships (Evans, 1986; Huggel et al., 2004; Kershaw et al., 2005) or calculated using empirical and physical models. Different types of dam breach and flood models have been applied to model glacial lake outburst scenarios and to assess potential downstream impacts (Bajracharya et al., 2007; Huggel et al., 2003; Mergili et al., 2011; Osti et al., 2012; Wang et al., 2008). For specific and local-scale scenario modeling the application of dynamic models is preferable to empirical models, as the latter represent an over-simplification of complex processes (Allen et al., 2009; Worni et al., 2012b). However, the large number of complex input parameters, the computational requirements and the topographic sensitivity of physically-based flood and dam breach models make dynamic GLOF modeling challenging.

Despite the existence of preliminary studies, little is known on the distribution and hazards of glacial lakes in the Indian Himalayas. Therefore the purpose of this study was (i) to provide a glacial lake inventory covering the entire Indian Himalayas and to prioritize lakes for further risk assessments; and (ii) to assess outburst probability and potential outburst magnitudes for three critical glacial lakes based on fieldwork and a sophisticated modeling approach. The two-dimensional dynamic BASEMENT model was used for this purpose as it allows simulation of cascades of complex processes which are typical for GLOFs.

2. Study regions

The Indian Himalayas have a glaciated area of about 23,300 km^2 (Philip and Sah, 2004), cover the northern boundary of India and span from west to east the states of Jammu and Kashmir (JK), Himachal Pradesh (HP), Uttarkhand (UK), Sikkim (SK) and Arunchal Pradesh (AP). Topography, morphology and climate vary significantly. Climate is influenced by the orographic barrier of the Himalayan mountain range in the north–south direction resulting in dry regions in the monsoon shadow. On the other hand, the Indian summer monsoon carries humidity from the Bay of Bengal into the eastern Himalayas but its influence weakens in the western portions of the range (Bookhagen and Burbank, 2006).

Based on a remote assessment of glacial lakes, as described in Section 3.2, three study sites were selected over the entire Indian Himalayas. The case study glacial lakes (Fig. 1) are located in different geographic regions and show contrasting climatic and topographic variability within the Indian Himalayas.

The first study site is located in the Zanskar mountain range which is aligned in parallel to the Indus valley on the plateau of Ladakh (JK). The crests of the mountain ranges are at 5400–5700 m a.s.l. on average, and reach maximum altitudes of 6000 m a.s.l. Rather small glaciers of 0.5–2 km^2 are common above 5100–5200 m a.s.l. (Burbank and Fort, 1985). The region of Ladakh lies north of the main Himalayan range and therefore escapes the full impact of the monsoon (Sant et al., 2011). The region is characterized by cool and arid climatic conditions. The Spong Togpo glacial lake (34°03′02″N; 76°43′04″E) is located in the Zanskar range at 5100 m a.s.l. some 26 km south of the village of Lamayuru. The Spong Togpo River reaches the first settlement (Honupatta village) 19 km downstream of the glacial lake and passes further small villages before discharging into the Yapola River (25 km) and finally into the Indus River some 50 km below the glacial lake.

The Lahaul–Spiti district (HP) comprises the NW–SE trending Pir Panjal and Great Himalaya mountain ranges, which are divided by the Chandra Valley. The valley bottom averages 3500 m a.s.l. and the surrounding steep and glaciated mountains reach altitudes above 6000 m a.s.l. The northern slopes of Pir Panjal and the Great Himalayan range lie in the monsoon–arid transition zone (Owen et al., 1997), and are alternately influenced by monsoon in summer and mid-latitude westerlies in winter (Wagnon et al., 2007). The Gopang Gath cirque glacier which is mainly fed from the steep north faces of Mount Gepang Goh (5870 m a.s.l.) is located in the Great Himalaya range 20 km east of the village Keylong. Its proglacial lake at 4100 m a.s.l. (32°31′38″N; 77°13′03″E) is the source of the steep Sissunala River which discharges into the Chandra River at Sissu village (3100 m a.s.l.), 10 km downstream of the glacial lake.

The state of SK is located between Nepal and Bhutan on the south-facing slopes of the Himalayan mountain range. The predominantly steep mountain topography ranges from 300 to 8598 m a.s.l. and encompasses the third highest mountain in the world (Mount Kanchenjunga). SK covers an area of about 7300 km^2 of which about 900 km^2 is covered by glaciers (Bhasin et al., 2002). Climate is strongly influenced by the monsoon with much precipitation from April to September and a dry period in winter. Extreme rain events are recorded periodically, causing major landslides and inundations (Bhasin et al., 2002; Krishna, 2005). The Shako Cho glacial lake (27°58′29″N; 88°36′58″E) is located at 5000 m a.s.l. and below the south face of Mount Kangchengyao (6889 m a.s.l.) in North SK. Shako Cho lake is 12 km northeast of Thangu village (3900 m a.s.l.), where the small tributary river from the lake discharges into Teesta River.

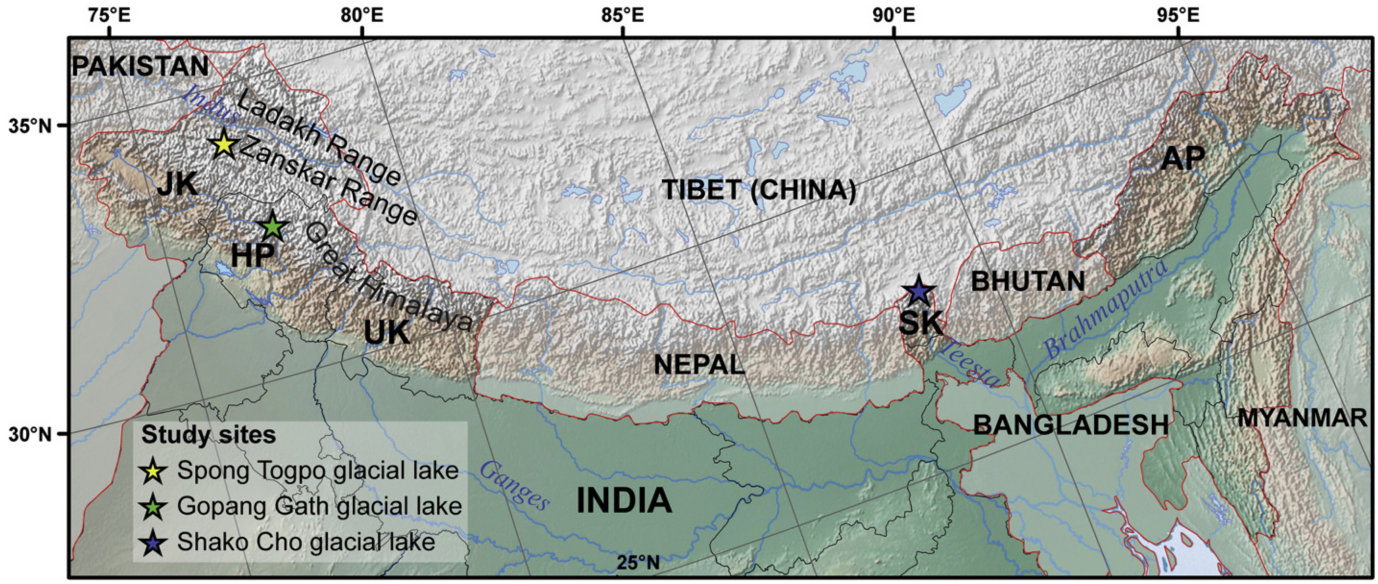

Fig 1. The Indian Himalayas at the northern boundary of India, with the case study sites of Spong Togpo glacial lake (Jammu and Kashmir, JK), Gopang Gath glacial lake (Himachal Pradesh, HP) and Shako Cho glacial lake (Sikkim, SK).

3. Data and methods

3.1. Data

LANDSAT ETM + imagery from 2000 to 2002 at 30-m resolution and high-resolution images from Google Earth (1.65 to 2.62-m resolution) were used for glacial lake mapping and lake classification. High-resolution images in Google Earth for areas of interest were mainly SPOT5 images of 2.5-m resolution, GeoEye images of 1.65-m resolution and Quickbird images of 2.62-m resolution. For Gopang Gath glacial lake a SPOT5 satellite image was available from 2010, and GeoEye satellite images (Google Earth) from 2011 and 2010 were used for Spong Togpo and Shako Cho glacial lakes, respectively.

Topography for the GLOF scenario modeling was obtained from the Global Digital Elevation Model (GDEM) version 2 of the Advanced Spaceborne Thermal Emission and Reflection Radiometer (ASTER), and from the digital elevation model (DEM) of the Shuttle Radar Topography Mission (SRTM). The spatial resolution of the ASTER GDEM v.2 is between 71 and 82 m; the absolute vertical accuracy was found to be within −0.2 m on average, with an accuracy of 17 m at the 95% confidence level (ASTER GDEM Validation Team, 2011). The resolution of the SRTM DEM is 90 m, with an elevation interval of 1 m. The indicated absolute and relative 90% horizontal accuracies are ±20 m and ±15 m, respectively, and the indicated absolute and relative 90% vertical accuracies are ±16 m and ±6 m, respectively (Strozzi et al., 2003).

3.2. Glacial lake mapping and classification

Glacial lakes were automatically mapped over the entire Indian Himalayas using the normalized difference water index (NDWI; Eq. (1)), applied on the spectral bands TM1 and TM4 of Landsat ETM + satellite images (Huggel et al., 2002).

$$\mathrm{NDWI} = \frac{\mathrm{TM4} - \mathrm{TM1}}{\mathrm{TM4} + \mathrm{TM1}}. \quad (1)$$

Subsequently, misclassified lakes were corrected through the visual postprocessing of data. Only lakes in close glacier proximity and with a surface area >0.01 km^2 were considered for the lake inventory. Based on remote sensing, lake-outburst probability was then assessed for all mapped lakes with available high resolution imagery in Google Earth. A qualitative approach was used by which four key indicators were assessed for each lake, namely: (i) *dam type*, (ii) *dam geometry* (iii) *freeboard* and (iv) *potential for lake impacts*. Thereby, each key indicator was assigned with one out of three possible attributes, indicating different lake outburst probabilities in the range of low, medium and high. The resulting matrix is used as a decision tool (Fig. 2) on which basis the expert can assign a general outburst probability for a lake (Huggel et al., 2004).

(i) *Dam type*: Moraine- and ice- dammed lakes may exhibit a high dam failure potential, whereas bedrock-dammed lakes are in general stable (Huggel et al., 2004). Lakes in flat topography in glacier forefields (often found in the Indian Himalayas west of Nepal) and without any clear dam structure are considered having low dam failure potential. Yet, lakes with rock dams or no dams can still present hazard situations in case of mass impacts into lakes that may cause overtopping waves. For these lakes the parameters (iii) *freeboard* and (iv) *potential for lake impacts* are critical for hazard assessments. Ice dammed lakes are practically inexistent in the Indian Himalayas and therefore not considered for this study. For moraine-dammed lakes (ii) *dam geometry*, (iii) *freeboard* and (iv) *potential for lake impacts* are crucial parameters. Parameters (ii) and (iii) influence hydraulic gradients within the moraine (Clague and Evans, 2000; Richardson and Reynolds, 2000a) (Fig. 2).

(ii) *Moraine dam geometry*: Moraine dams with high hydraulic gradients are more susceptible to collapses (Huggel et al., 2004). In addition, the dam width-to-height ratio, the width of the crest and the slope of the downstream face of moraine dams are an indication for the susceptibility of a moraine dam to fail (Huggel et al., 2004; Lu et al., 1999). In Fig. 2 critical values for these parameters are given in order to evaluate in a first-order assessment moraine dam stability.

(iii) *Freeboard*: The height of the freeboard is a crucial parameter for all dam types and must be considered in combination with the potential for lake impacts. The freeboard is a factor that influences whether a potential impulse wave will overtop the dam. Overtopping waves can lead to dam erosion and eventually to the failure of moraine dams. Even without partial or full failure of the glacial lake dam, overtopping waves may

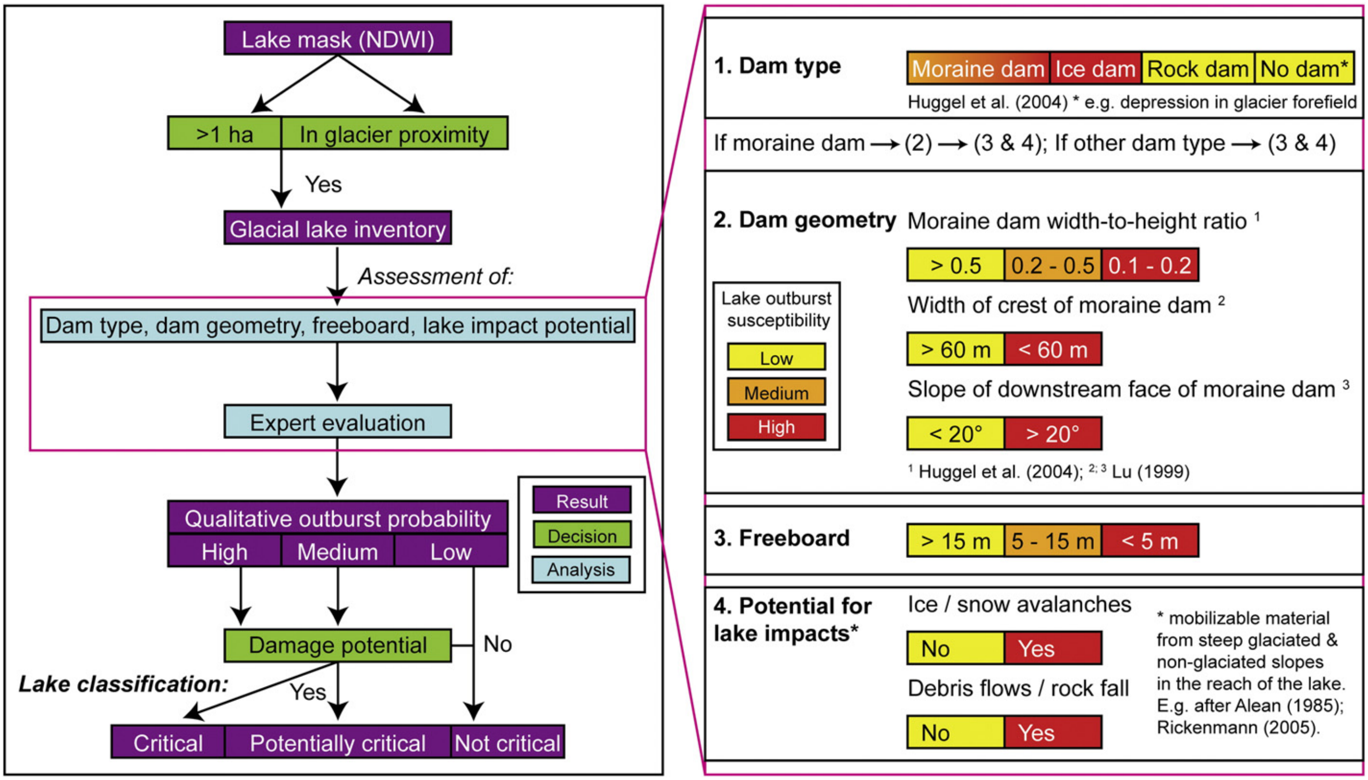

Fig. 2. Flow-chart illustrating the working steps of glacial lake detection based on the normalized difference water index (NDWI), lake-outburst probability assessment and lake classification in the Indian Himalayas.

travel valley downstream and cause inundation (Carey et al., 2012). The exact height of the freeboard is difficult to measure by remote sensing. This is why relatively rough freeboard values were defined to assess lake outburst susceptibilities (Fig. 2).

(iv) *Potential for lake impacts*: Impact waves from rock or ice falls, snow avalanches or debris flows have been observed to be most effective triggers for dam failure and lake outburst (Clague and Evans, 2000; Huggel et al., 2002; Richardson and Reynolds, 2000a). If steep glaciated and non-glaciated slopes or glacier tongues – i.e. potential sources for mass movements – are in reach of lakes, it is possible that impact waves could occur. Values for runout distances of different mass movements can be found e.g. in Alean (1985) or Rickenmann (2005) (Fig. 2).

Moraine-dammed lakes surrounded by steep slopes or exposed to glacier calving, with a significant potential for dam breach triggers, low freeboards and/or unstable dam geometries (i.e. low dam width-to-height ratio or a low width of dam crest or high slope of downstream face of dam) are considered to have high outburst probabilities. In the case of lakes for which at least one and up to four of the key parameters indicated moderate lake outburst potentials, the outburst probability was considered to be moderate as well. Low outburst probability is assigned for lakes for which all key parameters indicate low outburst susceptibility.

In addition to the qualitative outburst probability, we also considered damage potential (i.e. the exposure of infrastructure and inhabited areas) downstream of a lake for the classification of the detected lakes. The final result was a glacial lake inventory with mapped lakes categorized as: (i) *critical lakes* (ii) *potentially critical lakes*, (iii) *uncritical* lakes and (iv) *unclassifiable lakes* (i.e. lakes where high-resolution imagery was not available in Google Earth) (Fig. 2). *Critical* in this context does not necessarily imply that a lake is about to burst out, but that it should be of high priority for detailed field investigations and process modeling. *Potentially critical* lakes are of some priority, still requiring monitoring and possibly field reconnoitering. *Uncritical lakes* have a lower priority and are designated for periodic observation (sensu ICIMOD, 2011).

Based on this assessment, three *critical* moraine-dammed glacial lakes in different states of India and climatic regions of the Himalayas were selected from the lake inventory. For these lakes further investigations on outburst probability and potential outburst magnitude were carried out, based on field surveys and/or process modeling. The aim was to assess the risk emanating from these lakes, by evaluating the hazard potential (i.e. a function of outburst probability and magnitude) and the damage potential (i.e. a function of exposure and vulnerability). Damage potential was qualitatively assessed by field surveys and satellite image based surveys. For each downstream area of Spong Togpo-, Gopang Gath- and Shako Cho lake, damage potential was assigned to one of four categories, *low*, *moderate*, *high* and *very high* (refer to Fig. 10).

In September and November 2010, fieldwork was carried out at Spong Togpo and Gopang Gath glacial lakes. Sakho Cho glacial lake, in contrast, is located in the restricted area of North SK and could not therefore be visited. During the field campaigns further evidence was collected to assess lake-outburst probabilities and to obtain different model input parameters. On-site mapping of the lakes, moraines and outlet rivers was carried out using a GPS (Garmin GPSMAP 62STC) and a high-specification laser distance measurement device (Nikon LASER 550A S) with an integrated angle measurement function. These ground measurements, complemented by measurements from satellite imagery, helped to improve local topography of the model domains. Lake depth measurements in the proximity of the shore were performed with a sonar system (Humminbird Smartcast RF25) so as to gather data on lake bathymetry required for modeling.

3.3. Dynamic modeling

BASEMENT is a fluid dynamics and sediment transport model for the analysis of water-sediment flow propagation and breaching processes of non-cohesive earthen dam structures (Faeh et al., 2012). The two-dimensional program simulates water and sediment flows in a two phase system with separate unstructured meshes for the water and sediment phase. The computational meshes were created by the Surface Water Modeling System (SMS) software (SMS, 2012), based on the DEM of the study sites and field mapping, which also included lake bathymetry reconstruction. For the hydrodynamic calculations the program solves shallow water Eqs. (2) and (3) with an explicit finite-volume method and the application of an exact Riemann solver. The primary variables used are water depth h and specific discharge ($q = uh$, $r = vh$) in the coordinate directions.

$$\frac{\partial h}{\partial t}+\frac{\partial (uh)}{\partial x}+\frac{\partial (vh)}{\partial y}=0 \tag{2}$$

$$\begin{aligned}\frac{\partial}{\partial t}(hu)+\frac{\partial}{\partial x}\left(hu^2+\frac{1}{2}gh^2\right)+\frac{\partial}{\partial y}(huv)&=-gh\frac{\partial z_B}{\partial x}-\frac{\tau_{Bx}}{\rho}\\ \frac{\partial}{\partial t}(hv)+\frac{\partial}{\partial x}(huv)+\frac{\partial}{\partial y}\left(hv^2+\frac{1}{2}gh^2\right)&=-gh\frac{\partial z_B}{\partial y}-\frac{\tau_{By}}{\rho}\end{aligned} \tag{3}$$

where u is the velocity in x direction, v is the velocity in y direction, g is the gravitational acceleration, ρ is the fluid density, and z_B is the bottom elevation. Bed shear stresses ($\tau_{B,x}$, $\tau_{B,y}$) act in the direction of depth-averaged velocities and are determined using the quadratic resistance law with c_f being the dimensionless friction factor as

$$\tau_{Bx}=\rho\sqrt{u^2+v^2}u/{c_f}^2,\tau_{By}=\rho\sqrt{u^2+v^2}v/{c_f}^2. \tag{4}$$

Erosion and sediment transport of single and multiple grain classes caused by water flows are calculated with empirical sediment transport equations. The program evaluates surface erosion based on the bottom shear stress exerted by the flow on the inundated material. Within this study, the transport rate was determined using a modified Meyer-Peter and Müller (1948) formula (5) for fractional transport with the hiding function ξ after Ashida and Michiue (1971) and the critical bottom shear stress of incipient motion τ_{Bcr} from the Shields (1936) diagram. The hiding function considers effects of hiding and exposure of the grain particles with different sizes at fractional transport.

$$q_{Bg}=\beta_g\left(\frac{\tau_B-\xi_g\tau_{Bcr,g}}{0.25\rho}\right)^{3/2}\left(\frac{1}{(\rho_s/\rho-1)g}\right) \tag{5}$$

For dam breach modeling the lateral breach widening due to slope collapses of the side walls is considered with a geometrical 3D bank failure operator. It is based on three different critical failure angles: (i) one for dry or partially saturated material at the breach side walls above the water surface; (ii) one for bank material below the water surface; and (iii) one for deposited material resulting from slope collapses. If one of the failure angles is exceeded due to vertical erosion, gravitational bank failure occurs and the slope is flattened until the critical angles are reached. The material moves in downward direction of the cell's slope and is added to transport rates.

We applied BASEMENT to simulate a typical process chain of GLOFs, i.e. an (i) impulse wave generation by mass flows into the lake and wave propagation over the lake; (ii) dam overtopping and dam breaching; and (iii) lake emptying and flood propagation (Fig. 3). Model input parameters were either derived from field measurements, constituted typical (material) constants (Table 2) or based on a model calibration process as presented in Worni et al. (2012a). For glacial lakes with a high freeboard, smaller values for the calibration parameter *failure angle of deposition* had to be applied, in order to simulate realistic dam breaching mechanisms.

(i) *Impulse wave modeling*: Impulse wave generation was reproduced by a sudden release of mass flow from a potential mass-movement starting zone into the lake. The mass flow is represented by equivalent water flow, as solid mass movements cannot be adequately modeled in BASEMENT (Faeh, 2005). Momentum of the rapid and high-discharge flow is transferred to the lake water, whereby impulse waves develop. The impulse wave generation, propagation and run-up at the shore are described by shallow water equations, which represent an approximation, especially for the impulse wave generation. Water surface elevations of the lake and of the volume to be released into the lake were the initial conditions of the model in this case.

(ii) *Dam breach modeling*: Dam overtopping flow leads to vertical breach erosion. Sediment transport laws determine incision rates, which are controlled by the properties of the dam material and the shear stress of the water flow. Vertical breach incision leads to a steepening of the breach side walls, which collapse when the critical failure angles are exceeded. Due to breach enlargement, lake outflow increases. Breach expansion ceases when the lake level and outflow decrease below the threshold for bedload transport.

(iii) *Modeling flood propagation*: The water-sediment discharge resulting from the dam breach propagated valley downstream based on hydrodynamic and sediment transport calculations. Inundation depths, flow velocities, bottom shear stresses and changes in bed elevations are reported for each cell of the computational mesh.

For each case study small and large lake impact scenarios were modeled, for which two different volumes of water were released from potential avalanche starting zones into the lakes. The small scenarios represent minimum required lake impacts to trigger dam failure; they were determined by a trial-and-error approach. Thereby release volumes (initial conditions) were constantly increased until dam failure occurred in the simulation. The large scenarios were defined such as to cause significant lake overtopping with the consequence of larger breach formations, but still representing realistic lake impacts. Lake impacts were not quantified primarily by the impact volumes but by the momentum fluxes p into the lakes (see Eq. (6) for details). These represent the actual trigger pulses for wave generation, eventually leading to dam overtopping and dam breaching.

$$p=\int\rho\bullet Q\bullet v\bullet dt \tag{6}$$

where ρ is the density of water, Q is water discharge into the lake, v is velocity at lake impact and dt is the time step of constant water flow.

4. Results

4.1. Glacial lake inventory and glacial lake assessment

A total of 251 glacial lakes $>0.01\ km^2$ were identified and mapped over the Indian Himalayas of which 45 lakes are not classifiable due to missing high-resolution imagery in Google Earth. All other lakes were qualitatively classified according to outburst probability and damage potential. Based on the remote-sensing analysis, 12 lakes were considered as *critical* and will require in-depth field analysis and process modeling in the future so as to evaluate their hazard situation in greater detail. Another 93 lakes were considered as *potentially critical* and 101 lakes were deemed to present no GLOF risk to downstream locations under present conditions. *Critical lakes* were detected in the states of JK (2 lakes), HP (2) and SK (8). For each of these states

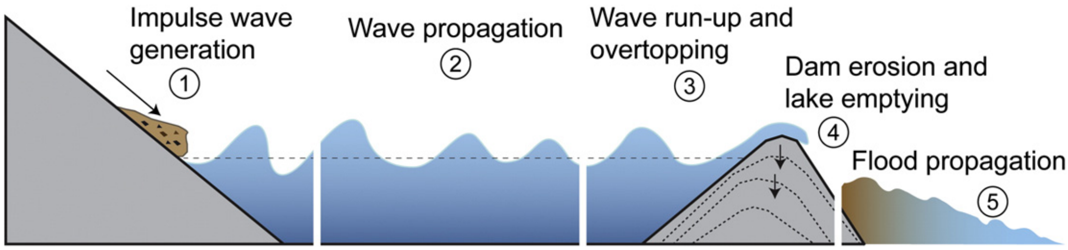

Fig. 3. Schematic sketch of cascading effects of a GLOF: The different phases 1–5 were simulated with the BASEMENT model at one stretch. The mass flow into the lake is represented by equivalent water flow (after Heller et al., 2008).

the lake with the highest GLOF risk was selected for a detailed hazard assessment (Fig. 4; Table 1).

The proglacial Spong Togpo lake in JK (Fig. 5A) was considered as *critical* principally due to its low freeboard, the downstream damage potential and the possibility for mass movements to occur from the steep lake environments. On-site reconnaissance revealed that the low freeboard (1 m), the low dam top width-to-height ratio (0.15) and the unconsolidated moraine material would probably cause dam erosion in the case of overtopping flows. Average measured lake depth (at 30 m from the shore) was ca. 12 m, and empiric relationships indicate an average lake depth of 15 m, resulting in a lake volume of ca. 2.3×10^6 m^3 (Table 2). The hanging glacier above the lake has an angle of reach of ca. 22°, a major ice avalanche would therefore reach the lake (Table 2.). In addition, retreat of the flat glacier behind the lake would cause lake growing, resulting in smaller and more frequent avalanches reaching the lake, since the angle of reach would increase in the case of glacier retreat. However, based on satellite imagery, the glacier tongue remained almost stationary

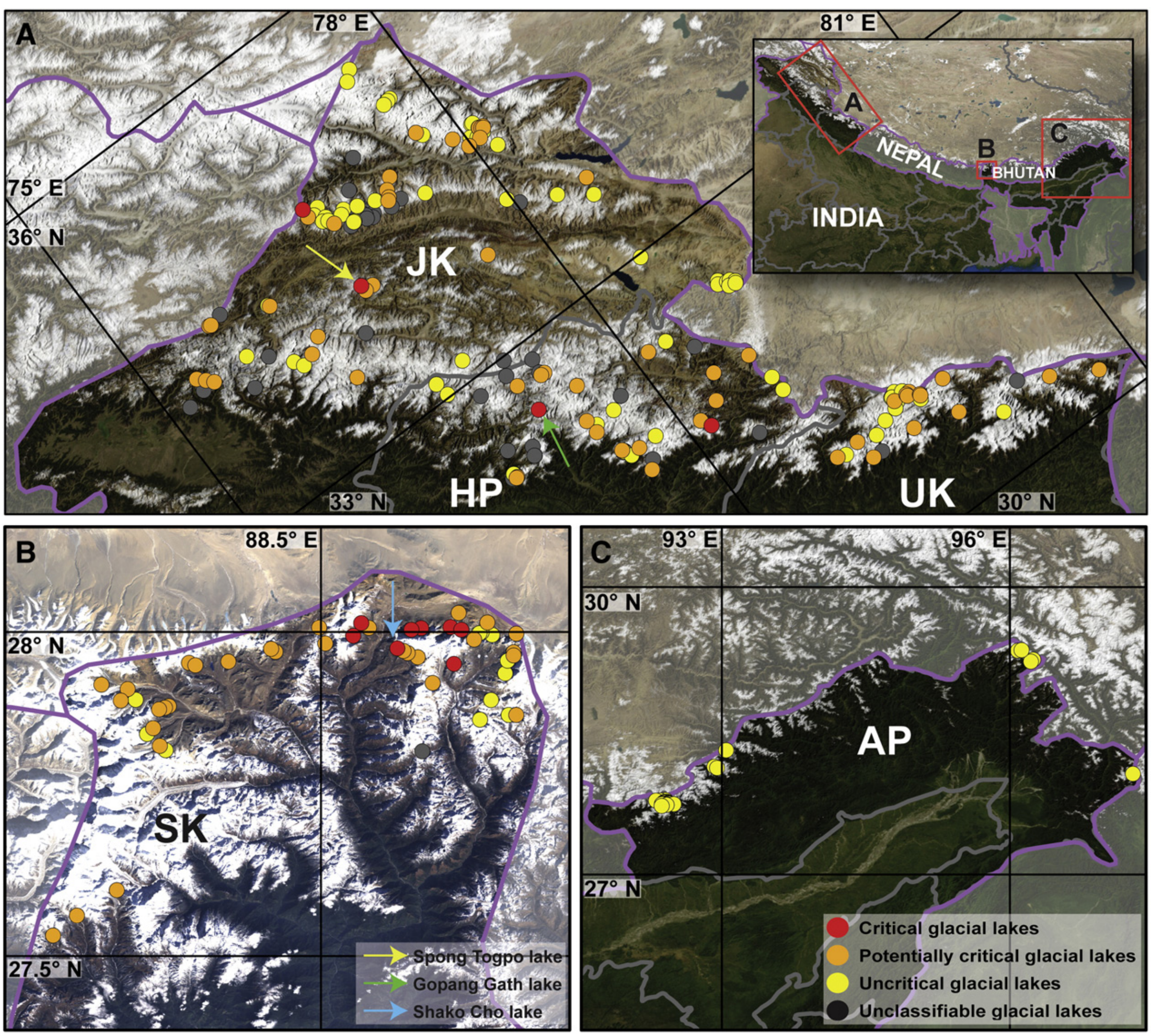

Fig. 4. Glacial lake inventory with mapped and classified glacial lakes over the entire Indian Himalayas. The coordinates of the mapped glacial lakes are given in Table 1. Three critical glacial lakes are indicated by arrows. For these lakes a detailed risk assessment has been carried out. The maps A, B and C illustrate three different regions within the Indian Himalayas (see inset in map A).

Table 1
Coordinates (long/lat) of mapped glacier lakes of Fig. 4 over the Indian Himalayas. Colors indicate *critical* (red), *potentially critical* (orange) and *uncritical* (yellow) lakes. Lakes for which no high-resolution imagery was available in Google Earth were not classified (gray). Bold black lines delimit Indian states, which are from left to right or west to east: JK, HP, UA, SK, and AP.

78°43'43"E 32°44'18"N	77°10'10"E 34°54'12"N	77°10'39"E 34°29'43"N	78°7'36"E 34°25'25"N	77°36'23"E 33°40'16 "N	77°3'0"E 34°25'34"N	76°16'56"E 33°31'38"N	76°55'54"E 32°52'0"N	76°47'15"E 32°13'17"N	79°29'13"E 30°58'49"N	78°59'10"E 30°44'56"N	88°12'7"E 27°54'43"N	88°44'39"E 27°59'54"N	88°25'47"E 27°58'11"N	92°25'8"E 27°45'33"N
78°29'56"E 32°58'31"N	77°14'24"E 34°50'59"N	76°59'31"E 34°29'26"N	77°15'22"E 34°26'12"N	77°13'33"E 32°58'29"N	76°4'33"E 34°21'7"N	78°16'18"E 32°21'56"N	77°24'2"E 32°51'15"N	76°46'47"E 32°13'18"N	79°27'33"E 30°58'32"N	78°46'15"E 30°54'38"N	88°11'29"E 27°53'39"N	88°44'9"E 27°59'18"N	88°25'23"E 27°58'26"N	92°23'41"E 27°45'20"N
78°11'54"E 32°56'40"N	77°43'27"E 34°43'1"N	78°7'6"E 34°28'0"N	78°4'8"E 34°24'52"N	78°30'12"E 33°33'26"N	76°5'1"E 34°20'26"N	77°45'41"E 32°14'33"N	77°11'41"E 32°45'44"N	77°39'17"E 32°11'23"N	79°22'9"E 30°58'22"N	78°50'0"E 30°53'19"N	88°15'56"E 27°53'8"N	88°47'48"E 27°57'50"N	88°12'51"E 27°53'43"N	92°24'5"E 27°45'16"N
78°51'3"E 32°29'32"N	77°45'15"E 34°40'25"N	78°7'12"E 34°27'54"N	77°6'53" E 34°25'43"N	76°58'58"E 33°9'33"N	75°19'30"E 34°14'1"N	78°25'5"E 32°12'15"N	77°22'57"E 32°44'41"N	77°29'35"E 32°10'47"N	79°27'40"E 30°57'49"N	79°6'8"E 30°52'0"N	88°15'33"E 27°52'59"N	88°45'44"E 27°53'42"N	88°21'25"E 27°57'16"N	92°26'4 3"E 27°45'10"N
78°50'10"E 32°28'9"N	77°4'14"E 34°40'26"N	77°4'4"E 34°29'2"N	78°4'51"E 34°23'59"N	76°42'36"E 34°45'55"N	75°22'28"E 34°11'5"N	78°24'56"E 31°57'53"N	77°24'43"E 32°43'19"N	77°27'26"E 32°8'1"N	79°20'0"E 30°56'33"N	79°13'8"E 30°54'58"N	88°15'1"E 27°52'51"N	88°47'21"E 27°52'20" N	96°5'0"E 29°20'17"N	92°26'29"E 27°44'42"N
78°54'9"E 32°26'43"N	76°57'7"E 34°35'5"N	78°8'52"E 34°27'25"N	77°58'48"E 34°23'57"N	76°48'26"E 34°42'48"N	75°43'21"E 34°8'40"N	78°42'8"E 31°54'45"N	77°22'59"E 32°43'14"N	77°31'36"E 31°54'54"N	78°57'28"E 30°54'41"N	88°42'43"E 28°1'45"N	88°14'28"E 27°51'6"N	88°48'4"E 27°52'19"N	96°14'39"E 29°14'39"N	92°23'15"E 27°44'38"N
78°55'28"E 32°26'29"N	77°22'15"E 34°34'19"N	78°9'4"E 34°27'25"N	77°5'23"E 34°24'33"N	76°42'29"E 34°41'46"N	75°24'58"E 34°8'17"N	77°38'24"E 31°51'5"N	77°12'55"E 32°31'39"N	77°32'18"E 31°53'56"N	79°32'28"E 30°54'57"N	88°33'43"E 28°0'49"N	88°13'55"E 27°50'33"N	88°44'41"E 27°51'53"N	96°13'8"E 29°13'31"N	92°25'57"E 27°44'35"N
78°57'10"E 32°24'46"N	76°49'2"E 34°34'4"N	76°58'13"E 34°28'40"N	77°20'19"E 34°23'39"N	76°45'0"E 34°40'55"N	75°18'55"E 34°8'9"N	77°47'20"E 31°50'58"N	77°32'52"E 32°29'53"N	77°31'32"E 31°53'53"N	79°32'25"E 30°54'30"N	88°39'16"E 28°0'22"N	88°15'5"E 27°49'27"N	88°39'21"E 27°48'57"N	96°7'25"E 29°20'41"N	92°26'41"E 27°44'31"N
78°53'47"E 32°24'41"N	76°54'57"E 34°33'45"N	77°2'45"E 34°28'31"N	77°14'54"E 34°23'10"N	76°48'45"E 34°37'11"N	75°51'15"E 34°2'48"N	78°18'21"E 31°47'22"N	76°59'7"E 32°16'22"N	77°31'56"E 31°53'52"N	79°44'47"E 30°54'30"N	88°29'49"E 28°0'25"N	88°15'38"E 27°49'3"N	88°40'19"E 27°55'16"N	97°16'58"E 28°3'13"N	92°25'24"E 27°44'19"N
78°56'48"E 32° 23'57"N	77°2'56"E 34°32'36"N	78°8'4"E 34°27'14"N	77°30'36"E 34°19'0"N	76°46'38"E 34°36'23"N	75°37'54"E 33°55'21"N	78°7'29"E 31°44'21"N	76°50'53"E 32°25'17"N	77°33'39"E 31°50'33"N	79°31'29"E 30°53'8"N	88°41'58"E 28°0'27"N	88°11'6"E 27° 36'7"N	88°42'17"E 27°57'3"N	93°2'42"E 28°17'55"N	92°22'26"E 27°44'12"N
77°36'41"E 35°23'13"N	78°5'29"E 34°31'15"N	78°8'40"E 34°26'47"N	78°9'20"E 34°16'52"N	76°48'47"E 34°35'10"N	75°58'42"E 33°54'12"N	77°40'7"E 31°43'23"N	78°7'16"E 32°22'47"N	76°43'14"E 33°7'59"N	79°21'25"E 30°44'37"N	88°42'58"E 28°0'13"N	88°7'25"E 27°33'46"N	88°38'21"E 28°0'13"N	92°55'25"E 28°7'44"N	92°29'57"E 27°44'14"N
77°32'36"E 35°19'29"N	78°6'4"E 34°31'13"N	76°57'48"E 34°28'1"N	76°43'2"E 34°3'9"N	76°59'48"E 34°30'24"N	76°7'10"E 33°52'5"N	77°37'7"E 31°39'57"N	77°0'48"E 32°20'10"N	76°44'34"E 33°1'26"N	79°41'40"E 30°38'21"N	88°48'3"E 27°59'51"N	88°5'13"E 27°31'54"N	88°38'56"E 27°57'40"N	92°57'5"E 28°6'54"N	92°25'31"E 27°43' 43"N
77°43'14"E 35°2'11"N	76°50'2"E 34°32'34"N	78°1'30"E 34°26'41"N	76°47'16"E 34°0'24"N	76°59'48"E 34°30'24"N	76°1'18"E 33°50'10"N	78°44'31"E 31°40'42"N	76°59'4"E 32°16'24"N	79°23'59"E 31°2'46"N	80°10'37"E 30°33'51"N	88°37'3"E 27°58'30"N	88°47'2"E 27°56'10"N	88°38'1"E 27°58'3"N	92°24'52"E 27°46'48"N	92°22'15"E 27°43'2"N
77°41'27"E 35°1'55"N	77°54'42"E 34°30'43"N	76°57'28"E 34°27'57"N	78°1'39"E 33°50'24"N	75°45'3"E 34°30'43"N	76°31'52"E 33°45'8"N	78°10'6"E 31°39 '39"N	76°46'40"E 32°15'21"N	79°21'22"E 31°1'25"N	80°23'20"E 30°26'45"N	88°47'49"E 27°58'7"N	88°47'15"E 27°57'21"N	88°37'37"E 27°58'15"N	92°21'11"E 27°46'36"N	
77°41'55"E 35°1'55"N	77°17'50"E 34°30'21"N	76°57'46"E 34°27'59"N	78°17'3"E 33°43'8"N	75°38'13"E 34°29'39"N	76°14'0"E 33°56'42"N	78°45'3"E 31°33'12"N	77°26'52"E 32°14'42"N	79°21'40"E 31°1'24"N	80°42'47"E 30°15'49"N	88°17'47"E 27°57'9"N	88°45'23"E 28°0'52"N	88°34'25"E 28°0'23"N	92°18'51"E 27°46'24"N	
77°39'34 "E 35°1'29"N	77°1'57"E 34°30'28"N	77°16'30"E 34°27'15"N	78°32'5"E 33°41'26"N	75°39'0"E 34°29'26"N	76°43'19"E 34°0'20"N	78°25'13"E 31°24'11"N	76°47'12"E 32°14'37"N	79°26'57"E 31°0'49"N	79°57'37"E 30°26'17"N	88°18'22"E 27°56'55"N	88°45'49"E 27°59'43"N	88°32'58"E 27°59'39"N	92°25'33"E 27°45'48"N	
77°11'25"E 34°58'27"N	77°4'6"E 34°29'56"N	76°55'24"E 34°27'13"N	77°57'54"E 33°54'53"N	77°3'31"E 34°27'3"N	75°9'38"E 34°5'40"N	77°10'25"E 32°52'19"N	76°45'10"E 32°14'1"N	79° 21'34"E 30°59'26"N	79°3'45"E 30°44'51"N	88°9'41"E 27°55'8"N	88°44'50"E 27°59'58"N	88°30'24"E 27°58'56"N	92°24'12"E 27°45'38"N	

over the past 10 years. In addition, it is possible that calving processes into the lake could initiate dam erosion with subsequent breaching processes. The same phenomenon can be initiated by heavy cloudbursts, such as observed in August 2010, when lake overtopping resulted in the formation of a 2-m deep breach. However, the fact that this exceptionally intense cloudburst did not cause a complete dam failure also indicates that a more significant trigger might be needed to effectively drain the lake.

The proglacial Gopang Gath lake in HP (Fig. 5B) was considered as *critical* principally due to the steep slope of the downstream face of the moraine dam, the big lake area and the possibility for mass movements to occur from the surroundings of the lake. The dam is of variable geometry and incised at its northern end by an outlet river. The river flows at low descent around the moraine dam, which renders it somewhat less susceptible to breach drastically. However, a significant overtopping flow could erode the dam also at its southern end, where the dam width-to-height ratio is lower but the freeboard is still at 5 m (Table 2). Measurements taken at 30 m from the shore suggest average lake depths of ca. 30 m, and empiric relationships indicate an average lake depth of 27 m, resulting in a lake volume of ca. 15.7×10^6 m^3 (Table 2). Mass movements and debris flows from the south-facing mountains could reach the lake (angle of reach: 27°). At present, ice avalanches from the north-facing hanging glaciers are considered unlikely to enter the lake (angle of reach = 13 − 8°, depending on the source area). In the past 10 years the flat glacier behind the lake retreated by 300 m and further lake growing is probable to occur in the future. Hence, ice avalanches from the hanging glaciers could more easily reach the lake in the future. Calving activities of the massive glacier tongue entering the lake represent yet another possible trigger of dam breach processes.

The large proglacial Shako Cho lake in SK (Fig. 5C) was considered as highly *critical* due to the following key indicators: low width-to-height ratio of the end moraine, which consists of loose and granular material; the steep, glaciated, 1000-m high mountain face rising above the lake; and the position of Thangu village to the river flowing out of the lake. Although fieldwork could not be carried out in this case, photographs of the lake and dam as well as high-resolution satellite imagery were readily available to assess the hazard situation. Empiric relationships indicate an average lake depth of 27 m, resulting in a lake volume of ca. 15.5×10^6 m^3 (Table 2). Mass impacts into the lake from the mountain face above the lake appear likely and dam overtopping waves are possible, even at a freeboard of about 10 m (based on SRTM DEM measurements) (Table 2). An overtopping flow would likely lead to dam erosion due to the sharp dam geometry and weak dam structure. No armored lake outflow exists at present and lake drainage occurs through piping. Heavy earthquakes, as occurred in SK in September 2011 (magnitude 6.9), are yet another possible source for dam breach processes to be initiated at this lake.

4.2. Model results

The energies transferred to the lakes from the small and large impact scenarios are represented by the momentum fluxes and were calculated for the three case study lakes (Table 3). Table 3 also indicates lake impact volumes, which however, should not represent real impact volumes of typical mass movements, due to differences in immersion processes and densities between water (as modeled) and solids (e.g. ice, rock, debris).

4.2.1. Spong Togpo lake

The smaller lake impact scenario eroded a breach of 24 m depth and 60 m width into the end moraine. The lake level was lowered by 20 m and 2.4×10^6 m^3 water drained in 120 min with a maximal discharge of 1400 m^3 s^{-1}. Only 70 min after impulse wave generation the flood wave reached Honupatta with maximum flow velocities of 7 m s^{-1} and maximum flow depths of 7 m. Such a GLOF scenario would flood

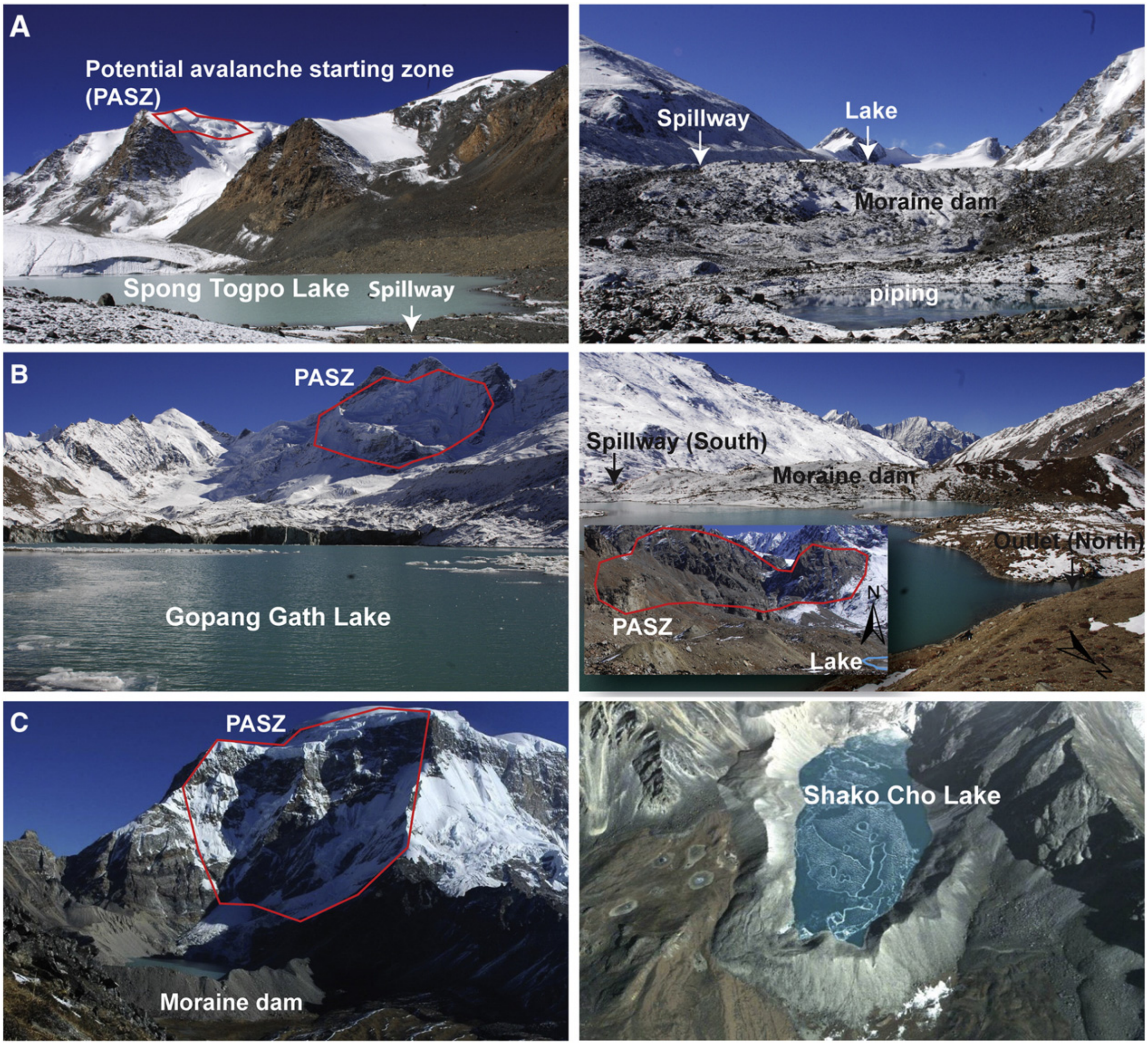

Fig. 5. Critical glacial lakes in JK, HP and SK represented with (A) Spong Togpo, (B) Gopang Gath and (C) Shako Cho lakes. Pictures were taken during fieldwork in September and November 2010. Pictures from Shako Cho lake were extracted from Google Earth (bird view) and obtained from a mountaineer (ground view). Potential ice avalanche starting zones (PASZ) are indicated. For Gopang Gath lake, there is also evidence for debris-flow activity from the south-facing mountains (inset).

mainly farm land close to the river, threatening farmers working in the fields and trekkers frequenting the area (Fig. 6).

In contrast, the large lake impact scenario eroded a breach of 22 m depth and 120 m width, and 3.6×10^6 m^3 water drained in 120 min. Maximum discharge was calculated at 4000 m^3 s^{-1} and the lake level was lowered by 17 m. The wide breach resulted in generally smaller lake outflow velocities than in scenario 1. As a consequence, bottom shear stresses were smaller, causing less vertical dam erosion and lake lowering. Some 50 min after mass-movement impact, the flood wave reached Honupatta village with maximum flow velocities of 9 m s^{-1} and maximum flow heights of 8 m. Such a GLOF would inundate farm land located next to the river and flood a local road at various instances. Houses of local residents are, in contrast, unlikely to be affected by the flood (Fig. 6).

4.2.2. Gopang Gath lake

The smaller lake impact scenario eroded the dam at its northern end (i.e. in the lake outlet area), ending up in maximal breach depths of 16 m. This would lead to total lake lowering of ca. 7 m and a release of 5.3×10^6 m^3 water in 180 min, with maximal discharge of 1250 m^3 s^{-1}. Some 50 min after the generation of the impact wave, the flood wave reached Sissu village with maximum flow velocities of 7 m s^{-1} and maximum flow depths of 6 m. Model results indicate that such a GLOF scenario would have minor effects in Sissu; only a ruin located next to the river would be inundated as well as some farmland upstream of the village. However, bridge foundation at the local road might be damaged (Fig. 7).

The larger lake impact scenario eroded the moraine dam at both its northern and southern ends. Final maximal breach depths were calculated to 20–27 m, and the lake was lowered by 13 m. The erosion of two breaches caused much stronger lake outflow and a total volume of 12.6×10^6 m^3 water was released in 180 min with maximal discharge of 3850 m^3 s^{-1}. Some 30 min after the lake impact, the flood wave reached Sissu with maximum flow velocities of 13 m s^{-1} and maximum flow depths of 10 m. Such a GLOF would have minor to moderate impacts in Sissu; two ruins located next to the river would be likely destroyed and a larger surface of farmland (as compared to scenario 1) would be flooded. Model results also suggest minor flooding in the village's periphery, but the DEM is inaccurate for the deep (25 m) and narrow (5–7 m) gorge below the bridge. It is likely that the flood would not leave the river channel here due to the strong incision; however, the bridge foundation could be

Table 2
Key parameters to characterize the three case study glacier lakes, to evaluate their outburst probabilities and to model outburst scenarios. Field measured (M), empiric (E), visually assessed (V), remote sensing and DEM-based assessed (R), assumed values (A) and (typical) material constants (C). *Model input parameters. For some key parameters the sources are referenced.

Parameter	Spong Togpo lake (1)	Gopang Gath lake (2)	Shako Cho lake (3)
Coordinates; altitude ($R_{1–3}$)	34°03′02″N; 76°43′04″E; 5100 m a.s.l.	32°31′38″N; 77°13′03″E; 4100 m a.s.l.	27°58′29″N; 88°36′58″E; 5000 m a.s.l.
Base axes; lake area ($R_{1–3}$)	620×300 m; 0.15 km^2	1700×500 m; 0.58 km^2	1420×520 m; 0.575 km^2
Mean lake depth ($E_{1–3}$); (Huggel et al., 2004)	15 m	27 m	27 m
Ø lake depth at 30 m ($M_{1,2}$)	12 m	30 m	–
Freeboard ($M_{1,2}$; R_3) (Huggel et al., 2004;)	1 m	North: 0 m South: 5 m	10 m
Dam material ($V_{1,2}$; R_3)	Non-cohesive, unconsolida-ted, poorly sorted, granular	Non-cohesive, unconsolida-ted, poorly sorted, granular	Non-cohesive, unconsolida-ted, poorly sorted, granular
Porosity* ($C_{1–3}$) (Parriaux and Nicoud, 1990)	15%	15%	15%
Manning's n of dam* ($C_{1–3}$) (USGS, 2012)	0.05	0.05	0.05
Dam width/height ($M_{1,2}$; R_3) (Huggel et al., 2004)	0.15	Northern end of dam: 0.6 Southern end of dam: 0.5	0.15
Dam top width ($M_{1,2}$; R_3) (Wang et al., 2008)	5 m	North: 10 m South: 10 m	10 m
Distal dam flank steepness ($M_{1,2}$; R_3); (Xin et al., 2008)	30°	North: 5–13° South: 30°	30°
Ice cored dam ($V_{1,2}$) (Yamada and Sharma, 1993)	No evidence	No evidence	–
Material failure angles of dam material* ($M_{1–2}$; A_3)	40° below-, 70° above water surface	33° below-, 70° above water surface	40° below-, 70° above water surface
Grain size distribution of dam material* ($M_{1–2}$; A_3) mm %	4 8 22 64 128 180 28 12 16 14 20 10	4 11 32 90 256 720 22 10 21 22 15 10	4 8 22 64 128 180 28 12 16 14 20 10
Angle of reach starting zone — lake ($R_{1–3}$)	22°	Ice fall: 13–18° debris flow: 27°	48°
Topography best represented with* ($V_{1–3}$)	SRTM DEM	ASTER GDEM v.2	SRTM DEM

damaged or even destroyed. It is likely that a large GLOF would affect the helicopter landing field and flood part of a water reservoir (Fig. 7).

4.2.3. Shako Cho lake

At Shako Cho lake, impact magnitudes had a less significant effect on dam breaching and lake emptying. (A significantly differing effect can only be achieved with unrealistically large lake impact scenarios). For the small and large impact scenarios maximal breach depths of 43 m and 45 m were obtained, respectively. Maximal breach widths were 140 m and 180 m for the small and large scenarios, respectively. The lake level was lowered in both scenarios by 32 m and about 16×10^6 m^3 water drained in 180 min with a maximal discharge of 6100 m^3 s^{-1} and 6950 m^3 s^{-1} for scenarios 1 and 2, respectively. For both scenarios the flood wave reached Thangu village about 50 min after lake impact with maximal flow velocities of 15 m s^{-1} and maximal flow depths of 12 m. About 12 min later the GLOF would have reached the village of Yathang 3.5 km below Thangu. Maximum flow velocities and flow depths were at Thangu calculated to 9 m s^{-1} and 9 m, respectively. Both villages would be hit by the GLOF, and damage would be particularly severe in Thangu. Parts of the road, three bridges, about 100 buildings and farmland would be flooded and partly destroyed in Thangu; and parts of the road, one bridge and about 30 buildings would be flooded and partly destroyed in Yathang (Fig. 8).

5. Discussion

5.1. Glacial lake inventory

Within this study, only lakes with a surface >0.01 km^2 were considered in the inventory, since smaller lakes were assumed not to present a relevant hazard potential to downstream locations (ICIMOD, 2011). This threshold is reasonable to cope with the large number of small lakes and helps to ensure efficient use of limited resources for on-site investigations and glacial lake monitoring. As the inventory is based on satellite imagery taken between 2000 and 2002, it represents the state of glacial lakes from that period. However, we assume that only a limited number of lakes >0.01 km^2 would have developed since then (Gardelle et al., 2011). On the other hand, all lakes detected on the ~10-year old images were still present on the high-resolution Google Earth images from 2010 to 2011, but glacial lake areas have indeed changed in some instances since the early 2000s.

The evaluation and classification of outburst probabilities of glacial lakes by remote sensing are challenging and different approaches have been presented in the literature (Huggel et al., 2004; McKillop and Clague, 2007a,b; Wang et al., 2011). The approach presented here considers previous studies and is efficient for analyzing a large number of lakes. Four key parameters and critical guiding values (Fig. 2) form the basis for the evaluation of the mapped glacier

Table 3
Momentum fluxes and impact volumes into the three case study glacier lakes. For each lake large and small dam breach trigger scenarios were modeled. Small scenarios represent minimal required lake impacts to trigger dam failure and were evaluated in a trial-and-error approach. Large scenarios provoke in each case significant dam breaching.

Scenarios	Spong Togpo		Gopang Gath		Shako Cho	
	Momentum flux [N · s]	Impact volume [m^3]	Momentum flux [N · s]	Impact volume [m^3]	Momentum flux [N · s]	Impact volume [m^3]
Large (2)	9.84×10^9	1,600,000	6.82×10^{10}	4,700,000	4.07×10^{10}	2,800,000
Small (1)	1.6×10^9	600,000	1.35×10^{10}	1,100,000	2.55×10^{10}	2,300,000

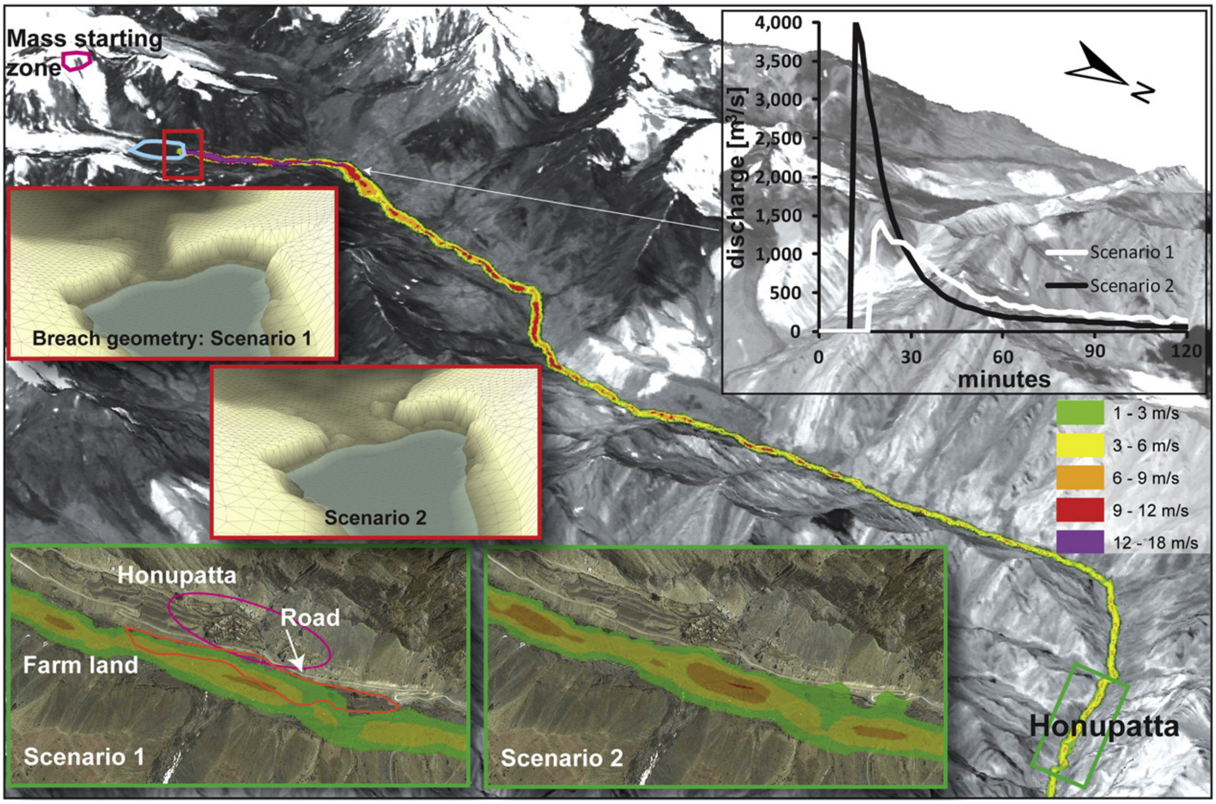

Fig. 6. Model results of small and large lake outburst scenarios for Spong Togpo glacial lake. The overview shows flow velocities of scenario 2. Included are the lake outburst hydrographs, breach geometries and flow velocities during a potential GLOF impact at Honupatta. Water was released into the lake from the mass-movement starting zone.

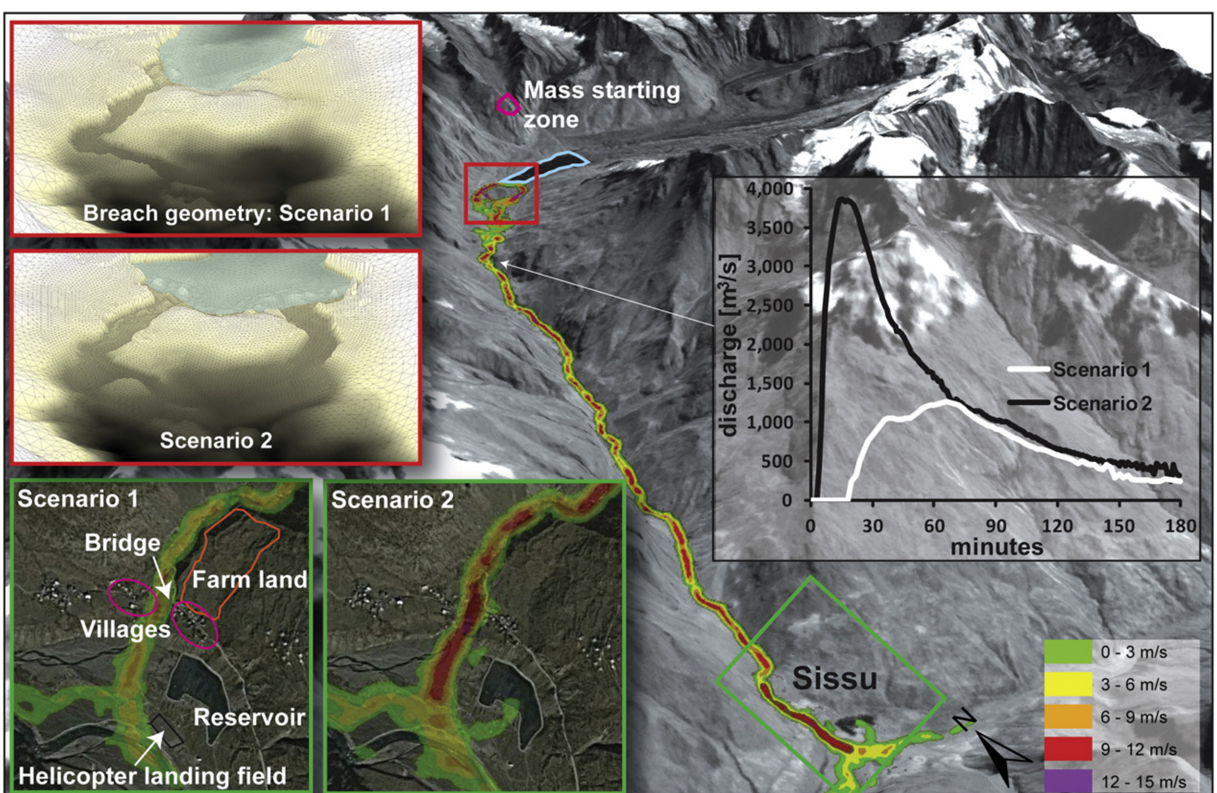

Fig. 7. Model results of small and large lake outburst scenarios for Gopang Gath glacial lake. The overview shows flow velocities of scenario 2. Included are the lake outburst hydrographs, breach geometries and flow velocities at Sissu. Water was released into the lake from the mass-movement starting zone.

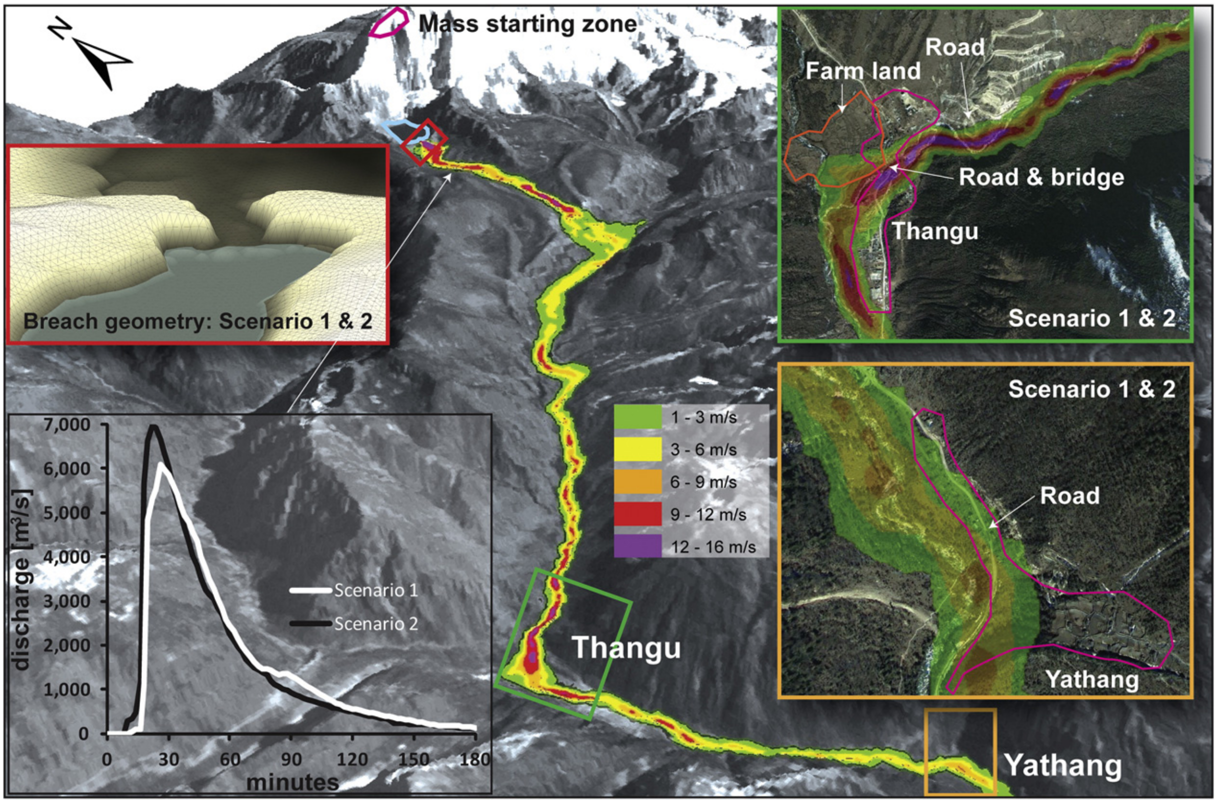

Fig. 8. Model results of small and big lake outburst scenarios for Shako Cho glacial lake. The overview shows flow velocities of scenario 2. Included are the lake outburst hydrographs, breach geometry and flow velocities at Thangu and Yathang. Water was released into the lake from the mass-movement starting zone.

lakes within the Indian Himalayas. Yet, expert knowledge on the stability of glacial lakes is required for the assessment, since analysis cannot only be based on the semi-quantitative decision tool, but also needs a holistic perspective and consideration of the dam, lake and lake surroundings.

The glacial lake inventory for the Indian Himalayas shows an overall trend for rather small and generally less critical glacial lakes when compared to other countries in the HKH such as e.g. Nepal or Bhutan (ICIMOD, 2010). Yet, a clear exception to this trend is the state of SK, where many large and (potentially) critical glacial lakes exist. Within the Indian Himalayas glacial lake distribution is more uniform in the glaciated areas of JK, HP, and UK (west of Nepal) than in SK, where glacial lake density is high, or in the case of AP, where lake distribution is very sparse. However, regional differences within the states can be substantial. The lake distribution pattern corresponds with lake characteristics in the different regions, which is also manifested in the number of *critical*, *potentially critical*, and *uncritical* lakes per state (Table 4).

Areas of all detected lakes are plotted in Fig. 9, illustrating again the remarkable situation in SK. Especially in North SK a high proportion of (very) large lakes exists, whereas in all other states medium to small lakes are dominant. Yet, the largest glacial lake in the Indian Himalayas is Samudra Tapu lake (77°32′52″E; 32°29′53″N) located in the Chandra Valley (HP) (Kulkarni et al., 2007). Two large lakes are located in the Karakoram mountain range of JK. UK and AP have, in contrast, very few and small lakes.

Beside a rather small number of lakes west of Nepal which should be monitored in the future, SK clearly represents a hotspot region in terms of possible GLOF occurrences, and more research and monitoring are urgently needed there. High-quality imagery in Google Earth indicates that moraine dams in SK very often have a low width-to-height ratio and that they consist of unconsolidated, granular

Table 4
Proportions of glacier lake counts per state in the Indian Himalayas, classified as *critical*, *potentially critical* and *uncritical*. The difference to 100% corresponds to *unclassifiable* lakes. (JK = Jammu and Kashmir, HP = Himachal Pradesh, UK = Uttarkhand, SK = Sikkim, AP = Arunchal Pradesh).

	JK	HP	UK	SK	AP
Tot # lakes	103	45	27	50	26
Critical	2%	4%	0%	16%	0%
Pot. critical	32%	36%	52%	60%	0%
Uncritical	41%	24%	40%	22%	96%

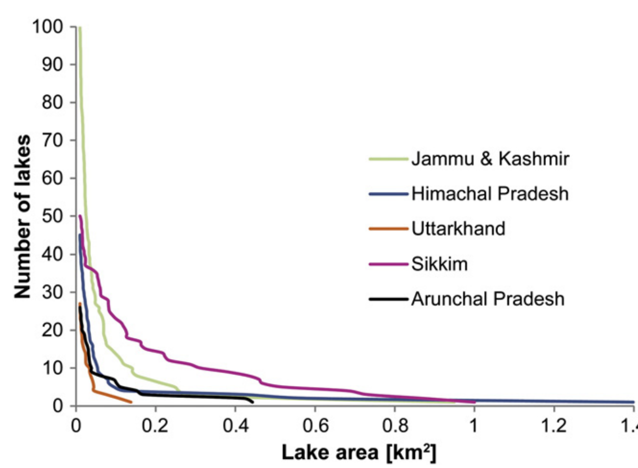

Fig. 9. Glacial lake areas of all mapped lakes in the Indian Himalayas, divided by states. The y-axis shows the number of lakes, and the x-axis illustrates lake areas. Sikkim has a high proportion of (very) large lakes, whereas rather small lakes prevail in the other states.

materials. As a result, they appear to be easily erodible by overtopping flows. Fujita (personal communication, February 2012) mapped and classified glacial lakes over large parts of the HKH and identified lakes which might potentially burst out with a volume $>10\times10^6$ m^3. Shako Cho lake is among the lakes mapped by Fujita and process modeling performed in this study clearly confirms that it should be considered as one of the most critical glacial lake in the Indian Himalayas.

5.2. Modeling

This study represents a pilot to model the chain of GLOF hazards, from mass-movement induced impact wave generation to dam breaching and flood propagation. The release volume and release location of the impacting mass define the GLOF scenario and are initial conditions of the model. Scenario definition is inherently affected by uncertainties, and we therefore defined small and large lake impact scenarios for each case study site, covering a reasonable range of potential dam breaches. We did not represent real lake impacts, since mass movements composed of ice and/or debris cannot be simulated with BASEMENT. In contrast, through the release of water volumes into the lake, we reproduced realistic impulse waves which have the potential to trigger dam breaches. This approach represents a sophisticated scenario definition, which is more accurate than any speculation about potential dam breach scenarios, where the shape of the breach and its enlargement over time must be assumed. However, the approach presented in this paper does not encompass all possible dam breach trigger mechanisms and does, for instance, ignore overtopping flows induced by extraordinary rainfalls.

Uncertainties, which may potentially affect model results, also existed in the definition of critical model input parameters and the DEM. The sediment transport components in the model have more limitations than the hydraulic components, as the former are based partly on empirical equations and geotechnical simplifications, and thus require several critical input parameters. The calibration of such critical input parameters based on similar past events is crucial, and was done in detail in a previous study on the basis of a moraine dam failure in the Patagonian Andes (Worni et al., 2012a). The resolution and accuracy of the DEM are correlated to the accuracy of model results (Wang et al., 2012), which is especially pronounced for advanced numerical models such as BASEMENT. Therefore a lack of recent and highly resolved elevation data from the Indian Himalayas remains a limiting factor in representing complex flow and dam breach dynamics (Allen et al., 2009). However, Wang et al. (2012) tested the influence of the SRTM DEM and ASTER GDEM version 1 data on hydraulic GLOF modeling in Tibet, and concluded that although flood inundation extent and water depths depend on the applied DEM, the level of deviation was of little significance when predicting high-discharge floods.

5.3. Risk assessment

Overtopping waves typically erode an initial breach into moraine dams. As soon as the initial breach depth is deeper than the lake freeboard, the hydrostatic lake pressure becomes the driving force for continuous breach enlargement and lake outflow. Hence, the smaller the freeboard, the less initial erosion is required to trigger dam failure, and the smaller a lake impact needs to be to effectively trigger a breach process. This correlation was confirmed with the GLOF modeling at Spong Togpo and Shako Cho lakes, but only partially for Gopang Gath lake. Although the freeboard at Gopang Gath lake was only 0–5 m, only massive lake impacts were resulting in significant dam failure (scenario 2). In this particular case, the limiting factor for moraine breaching was more related to dam geometry and only to a lesser extent to freeboard. Another reason for differences in dam breach processes is the mass impact location, which was at an angle of 90° with respect to the dam (whereas the angle was 180° at Spong Togpo and Shako Cho lakes). The impulse waves with the highest energy therefore hit the shore opposite of the impact location and the waves will have attenuated significantly by the time they reach the dam (Heller et al., 2008). Hence, in addition to freeboard, dam and lake geometry, mass impact location and direction have to be seen as other critical parameters regarding the impact magnitude required to trigger moraine dam failure. The key question to assess lake outburst probabilities is to decide whether the minimal lake impacts required to induce dam failure are realistic or not. The geotechnical aspect of the lake outburst probability assessment (i.e. the susceptibility of a dam to breach) was covered with the BASEMENT simulation.

The minimum momentum flux required to induce dam failure at Spong Togpo lake in JK was calculated to be about 1.6×10^9 Ns. An ice volume ($\rho_{ice}=917$ kg m^{-3}) of ca. 60,000–90,000 m^3 impacting instantly Spong Togpo lake with 30–20 m s^{-1}, respectively, would transfer the same momentum p ($p=mv$) to the lake, where m is the impact mass and v the impact velocity. Although such ice avalanches are plausible and not particularly extreme, little evidence for ice fall activity was found at the base of the hanging glacier at Spong Togpo lake during field surveys. However, warming may increase susceptibility of steep glaciers to fail (Huggel et al., 2010) and avalanches may occur at locations without precedence. Hence, moderate outburst magnitude and outburst probability have been assigned for Spong Togpo lake (Fig. 10).

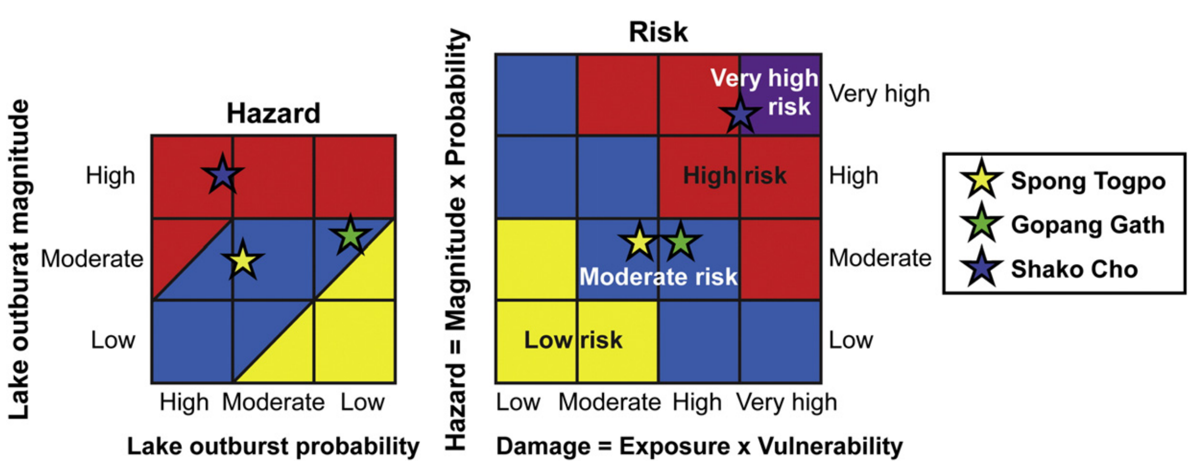

Fig. 10. Hazards and risks emanating from the three case-study glacial lakes were semi-quantitatively assessed, based on process modeling, field reconnaissance and remote sensing, and illustrated in a magnitude-probability and hazard-damage matrix.

If a debris flow ($\rho_{debris\ fl} = 2200$ kg m^{-3}) is assumed to trigger dam failure at Gopang Gath lake in HP, a sudden lake impact of 200,000–300,000 m^3 with velocities of 30–20 m s^{-1} would be required. Alternatively, an ice volume of 480,000–720,000 m^3 (assuming similar velocities) would result in 1.35×10^{10} Ns as well, which was found to be the minimum lake impact needed to trigger dam failure. Such volumes seem more realistic for ice avalanches than for debris flows, based on a visual judgment of potential source areas and evidence of past events. The occurrence of such ice avalanches reaching the lake with high velocities will become more likely to occur in the future with further glacier retreat. An ice impact volume of roughly $2–3 \times 10^6$ m^3 would be required to trigger a large (scenario 2) dam breach. Such trigger magnitudes are generally considered to be unlikely. As a consequence, a low outburst probability and a moderate outburst magnitude were finally chosen for Gopang Gath lake (Fig. 10).

Due to the steep terrain, potential ice impact velocities of 30–40 m s^{-1} were assumed for Shako Cho lake in SK. Ice impact volumes of 700,000–900,000 m^3 would transfer about 2.55×10^{10} Ns to the lake, which was found to be the minimal lake impact to induce dam failure. The highly glaciated, steep mountain faces above the lake clearly favor the occurrence of such an impact scenario. This results in a high outburst probability for Shako Cho lake and model results indicate high outburst magnitudes (Fig. 10).

Lake outburst probabilities were assigned for the three case study sites, based on the calculated mass impacts and the qualitative assessment of probability of occurrence of such mass movements: Spong Togpo lake was accordingly attributed a moderate outburst probability, Gopang Gath was considered to present a low outburst probability and Shako Cho was assigned to have a high outburst probability. Based on the modeled lake outburst hydrographs, the expected magnitudes of potential outburst floods are moderate for Spong Togpo and Gopang Gath lakes and high for Shako Cho lake (refer to chapter 4.2). Based on the modeled flow extents (Figs. 6–8), field surveys and the analysis of satellite imagery, the damage potential in Honupatta (JK) and Sissu (HP) was considered to be moderate, and high in Thangu (SK) and Yathang (SK). The semi-quantitative parameterization of lake-outburst probabilities, potential outburst magnitudes and damage potentials, was then used to qualitatively assess the risk for each lake as illustrated in Fig. 10.

6. Conclusion

In this study we followed a multi-level approach from basic detection of glacial lakes over large areas using LANDSAT imagery, an assessment of hazard potential of detected lakes based on high-resolution imagery, to local-scale risk assessments of individual lakes based on field evidence, remote sensing data and model output. So far, no glacial lake inventory existed for the entire Indian Himalayas, and therefore the contribution of a comprehensive inventory with mapped and classified glacial lakes is important for the identification of potential hazard sources and for the planning of adequate coping strategies. The existence of Spong Togpo and Gopang Gath lakes is hardly known to local people and therefore awareness building in villages downstream of critical glacial lakes should become a priority. The glacial lake inventory is also the basis for further analysis of priority lakes. The schemes used for the three lakes of this study can serve as a reference for the risk assessment at other lakes in the Indian Himalayas. Whereas ground observations remain crucial, novel modeling capabilities have been shown to be highly relevant for integral glacial lake assessments. Despite prevailing uncertainties in the modeling process the dynamic BASEMENT model has been demonstrated to be a valuable tool to assess lake-outburst probabilities and potential lake outburst magnitudes. Such data facilitates the planning and dimensioning of accurate mitigation measures in the form of e.g., early warning systems, and helps the justification of decisions aimed at preventing infrastructure and populated areas from being possibly at risk. Yet, apart from potential hazard sources, glacial lakes can also have a touristic potential (e.g. Samudra Tapu lake in the Chandra Valley, HP), and when considering glacial lake patterns and characteristics over large regions, glacial lakes can be used as an indirect indicator of glacier change.

Acknowledgments

We would like to thank Ashvin Gosain, Sandhya Rao and Prataph Singh from IIT Delhi (India) for administrative support and for providing data for this study. The mountain guides Prashant Mierupa and Tenzin Punchok were indispensable during fieldwork. This study was realized within the EU-FP7 project “HighNoon”.

References

Alean J. Ice avalanches: some empirical information about their formation and reach. J Glaciol 1985;31(109):324–33.
Allen SK, Schneider D, Owens IF. First approaches towards modelling glacial hazards in the Mount Cook region of New Zealand's Southern Alps. Nat Hazards Earth Syst Sci 2009;9:481–99.
Ashida K, Michiue M. An investigation over river bed degradation downstream of a dam. Proceedings 14th Congress of IAHR. Paris, France; 1971. p. 247–56.
ASTER GDEM Validation Team. ASTER Global Digital Elevation Model Version 2 — Summary of Validation Results. http://www.ersdac.or.jp/GDEM/ver2Validation/Summary_GDEM2_validation_report_final.pdf2011. [accessed 20 April 2012].
Babu-Govindha-Raj K. Remote sensing based hazard assessment of glacial lakes: a case study in Zanskar basin, Jammu and Kashmir, India. Geomatics, Nat Hazards Risk 2010;1(4):339–47.
Bajracharya B, Shrestha AB, Rajbhandari L. Glacial Lake outburst floods in the Sagarmatha Region. Mt Res Dev 2007;27(4):336–44.
Bhargava ON. Geology, environmental hazards and remedial measures of the Lunana area, Gasa Dzongkhag: report of 1995 Indo-Bhutan Expedition. Kolkata: Geological Survey of India; 1995.
Bhasin R, Grimstad E, Larsen JO, Dhawan AK, Singh R, Verma SK, et al. Landslide hazards and mitigation measures at Gangtok, Sikkim Himalaya. Eng Geol 2002;64(4):351–68.
Bolch T, Buchroitner M, Peters J, Baessier M, Bajracharya S. Identification of glacier motion and potentially dangerous glacial lakes in the Mt. Everest region/Nepal using spaceborne imagery. Nat Hazards Earth Syst Sci 2008;8:1329–40.
Bolch T, Kulkarni A, Kääb A, Huggel C, Paul F, Cogley JG, et al. The state and fate of Himalayan glaciers. Science 2012;336(6079):310–4.
Bookhagen B, Burbank D. Topography, reflief, and TRMM-derived rainfall variations along the Himalaya. Geophys Res Lett 2006;33:L08405.
Burbank DW, Fort M. Bedrock control on glacial limits: example from the Ladakh and Zanskar ranges; north-western Himalaya. India J Glaciol 1985;31(108):143–9.
Carey M. Living and dying with glaciers: people's historical vulnerability to avalanches and outburst floods in Peru. Global Planet Change 2005;47(2–4):122–34.
Carey M, Huggel C, Bury J, Portocarrero C, Haeberli W. An integrated socio-environmental framework for climate change adaptation and glacier hazard management: Lessons from Lake 513, Cordillera Blanca, Peru. Clim Change 2012;112:733–67.
Clague JJ, Evans SG. A review of catastrophic drainage of moraine-dammed lakes in British Columbia. Quat Sci Rev 2000;19:1763–83.
Costa JE, Schuster RL. The formation and failure of natural dams. Geol Soc Am Bull 1988;100:1054–68.
Evans SG. The maximum discharge of outburst floods caused by the breaching of man-made and natural dams. Can Geotech J 1986;23:385–7.
Faeh R. In: Minor H-E, editor. Numerik an der VAW: Entwicklungen und Beispiel des Triftgletschers. VAW-MitteilungZürich: ETH Zürich; 2005. p. 187–200.
Faeh R, Mueller R, Rousselot P, Veprek R, Vetsch D, Volz C, et al. BASEMENT — Basic Simulation Environment for Computation of Environmental Flow and Natural Hazard Simulation. VAW, ETH Zurich; 2012. www.basement.ethz.ch [accessed 20 April 2012].
Fujita K, Suzuki R, Nuimura T, Sakai A. Performance of ASTER and SRTM DEMs, and their potential for assessing glacial lakes in the Lunana region, Bhutan Himalaya. J Glaciol 2008;54(185):220–8.
Fujita K, Sakai A, Nuimura T, Yamaguchi S, Sharma RR. Recent changes in Imja Glacial Lake and its damming moraine in the Nepal Himalaya revealed by in-situ surveys and multi-temporal ASTER imagery. Environ Res Lett 2009;4:045205. http://dx.doi.org/10.1088/1748-9326/4/4/045205.
Gardelle J, Arnaud Y, Berthier E. Contrasted evolution of glacial lakes along the Hindu Kush Himalaya mountain range between 1990 and 2009. Global Planet Change 2011;75:47–55.
Heller V, Hager WH, Minor H-E. Rutscherzeugte Impulswellen in Stauseen Grundlagen und Berechnung. In: Minor H-E, editor. VAW-Mitteilung, 206. Zürich: ETH Zürich; 2008.
Hewitt K. Natural dams and outburst floods of the Karakoram Himalaya. In: Glen JW, editor. Hydrological aspects of alpine and high mountain areas. Association of Hydrological Sciences (IAHS); 1982. p. 259–69.
Huggel C, Kääb A, Haeberli W, Teysseire P, Paul F. Remote sensing based assessment of hazards from glacier lake outbursts: a case study in the Swiss Alps. Can Geotech J 2002;39(2):316–30.

Huggel C, Kääb A, Haeberli W, Krummenacher B. Regional-scale GIS-models for assessment of hazards from glacier lake outbursts: evaluation and application in the Swiss Alps. Nat Hazards Earth Syst Sci 2003;3:647–62.

Huggel C, Haeberli W, Kääb A, Bieri D, Richardson S. An assessment procedure for glacial hazards in the Swiss Alps. Can Geotech 2004;41:1068–83.

Huggel C, Fischer L, Schneider D, Haeberli W. Research advances on climate-induced slope instability in glacier and permafrost high-mountain environments. Geogr Helv 2010;65(2):146–56.

ICIMOD. Formation of Glacial Lakes in the Hindu Kush-Himalayas and GLOF Risk Assessment. http://www.unisdr.org/files/14048_ICIMODGLOF.pdf2010. [accessed 20 April 2012].

ICIMOD. Glacial Lakes and Glacial Lake Outburst Floods in Nepal. http://books.icimod.org/index.php/search/publication/7502011. [accessed 20 April 2012].

Kershaw JA, Clague JJ, Evans SG. Geomorphic and sedimentological signature of a two-phase outburst flood from moraine-dammed Queen Bess Lake, British Columbia, Canada. Earth Surf Process Landforms 2005;30:1-25.

Komori J. Recent expansions of glacial lakes in the Bhutan Himalayas. Quat Int 2008;184:177–86.

Korup O, Tweed F. Ice, moraine, and landslide dams in mountainous terrain. Quat Sci Rev 2007;26:3406–22.

Krishna AP. Snow and glacier cover assessment in the high mountains of Sikkim Himalaya. Hydrol Process 2005;19:2375–83.

Kulkarni AV, Bahuguna IM, Rathore BP, Singh SK, Randhawa SS, Sood RK, et al. Glacial retreat in Himalaya using Indian Remote Sensing satellite data. Curr Sci India 2007;92(1):69–74.

Lu R, Tang B, Li D. Introduction of debris flow resulted from glacial lakes failed. In: Lu R, Tang B, Zhu P, editors. Debris flow and environment in Tibet [in Chinese]. Chengdu, China: Sichuan University Publishing House; 1999. p. 69-105.

Malone E. Changing glaciers and hydrology in Asia: addressing vulnerabilities to glacier melt impacts. Washington: USAID; 2010. Available at: http://www.usaid.gov/locations/asia/documents/Asia_Glacier_Melt_Vulnerability_Nov-2010.pdf [Accessed 20 April 2012].

Massey C, Manville V, Hancox GT, Keys HJR, Lawrence C, McSaveney MJ. Out-burst flood (lahar) triggered by retrogressive landsliding, 18 March 2007 at Mt. Ruapehu, New Zealand — a successful early warning. Landslides 2010;7:303–15.

McKillop RJ, Clague JJ. Statistical, remote sensing-based approach for estimating the probability of catastrophic drainage from moraine-dammed lakes in southwestern British Columbia. Global Planet Change 2007a;56:153–71.

McKillop RJ, Clague JJ. A procedure for making objective preliminary assessments of outburst flood hazard from morainedammed lakes in southwestern British Columbia. Nat Hazards Earth Syst Sci 2007b;41:131–57.

Mergili M, Schneider D, Worni R, Schneider JF. Glacial Lake outburst Floods (GLOFs): challenges in prediction and modelling. Proceedings of the 5th International Conference on Debris-Flow Hazard Mitigation: Mechanics, Prediction and Assessment, Padua, Italy, 14—7 June; 2011. p. 973–82.

Meyer-Peter E, Müller R. Formulas for bed-load transport. Int Assoc Hydrol, Res, 2nd Congr Proc, Stockholm; 1948. p. 39–64.

Osti R, Egashira S. Hydrodynamic characteristics of the Tam Pokhari Glacial Lake outburst flood in the Mt. Everest region, Nepal. Hydrol Process 2009;23:2943–55.

Osti R, Egashira S, Adikari Y. Prediction and assessment of multiple glacial lake outburst floods scenario in Pho Chu River basin, Bhutan. Hydrol Process 2012. http://dx.doi.org/10.1002/hyp.8342.

Owen LA, Bailey RM, Rhodes EJ. Style and timing of glaciation in the Lahul Himalaya, northern India: a framework for reconstructing late Quaternary palaeoclimatic change in the western Himalayas. J Quat Sci 1997;12(2):83-109.

Parriaux A, Nicoud GF. Hydrological behaviour of glacial deposits in mountainous areas. Hydrol Mt Areas IAHS 1990;190:291–311.

Philip G, Sah MP. Mapping repeated surges and retread of glaciers using IRS-1C/1D data: a case study of Shaune Garang glacier, northwestern Himalaya. Int J Appl Earth Obs 2004;6:127–41.

Pitman EB, Patra AK, Kumar D, Nishimura K, Komori J. Two phase simulations of glacier lake outburst flows. J Comput Sci 2012. http://dx.doi.org/10.1016/j.jocs.2012.04.007.

Randhawa SS, Sood RK, Rathore BP, Kulkarni AV. Moraine-dammed lakes study in the Chenab and the Satluj River basins using IRS data. J Indian Soc Remote Sens 2005;33(2):285–90.

Richardson SD, Reynolds JM. An overview of glacial hazards in the Himalayas. Quat Int 2000a;65(66):31–47.

Richardson SD, Reynolds JM. Degradation of ice-cored moraine dams: implications for hazard development. In: Nakawo M, Raymond CF, Fountain A, editors. Debris-covered GlaciersIAHS Red Book series; 2000b. p. 187–98.

Rickenmann D. Runout prediction methods. In: Jakob M, Hungr O, editors. Debris-flow hazards and related phenomena. Berlin/Heidelberg: Springer; 2005. p. 305–24.

Sant AS, Wadhawan SK, Ganjoo RK, Basavaiah N, Sukumaran P, Bhattacharya S. Morphostratigraphy and Palaeoclimate Appraisal of the Leh Valley, Ladakh Himalayas, India. J Geol Soc India 2011;77:499–510.

Shields A. Anwendung der Aehnlichkeitsmechanik und der Turbulenzforschung auf die Geschiebebewegung. Mitt Nr 87. Berlin: Versuchsanstalt für Wasser- und Schiffbau; 1936.

SMS. http://www.scisoftware.com/products/sms_details/sms_details.html. 2012. [accessed 20 April 2012].

Strozzi T, Wegmuller U, Wiesmann A, Werner C. Validation of the X-SAR SRTM DEM for ERS and JERS SAR geocoding and 2-pass differential interferometry in alpine regions. Geoscience and Remote Sensing Symposium, 2003, vol. 1. IGARSS '03. Proceedings, 2003 IEEE International; 2003. p. 109–11.

Tashi T. Preliminary report on the investigation of glacial lakes at Pho Chhu source and the assessment of food affected areas in Lunana. Thimphu: Royal Bhutanese Government; 1994.

USGS. Verified roughness characteristics of natural channels. http://wwwrcamnl.wr.usgs.gov/sws/fieldmethods/Indirects/nvalues/index.htm2012. [accessed 20 April 2012].

Vuichard D, Zimmermann M. The Langmoche flash-flood, Khumbu Himal, Nepal. Mt Res Dev 1986;6(1):90–4.

Wagnon P, Linda A, Arnaud Y, Kumar R, Sharma P, Vincent C, et al. Four years of mass balance on Chhota Shigri Glacier, Himachal Pradesh, India, a new benchmark glacier in the western Himalaya. J Glaciol 2007;53(183):603–11.

Wang X, Shiyin L, Wanqin G, Junli X. Assessment and simulation of glacier lake outburst floods for Longbasaba and Pida Lakes, China. Mt Res Dev 2008;28(3/4):310–7.

Wang W, Yao T, Gao Y, Yang X, Kattel DB. A first-order method to identify potentially dangerous glacial lakes in a region of the southeastern Tibetan Plateau. Mt Res Dev 2011;31(2):122–30.

Wang W, Yang X, Yao T. Evaluation of ASTER GDEM and SRTM and their suitability in hydraulic modelling of a glacial lake outburst flood in southeast Tibet. Hydrol Process 2012;26:213–25.

Worni R, Stoffel M, Huggel C, Volz C, Casteller A, Luckman BH. Analysis and dynamic modeling of a moraine failure and glacier lake outburst flood at Ventisquero Negro, Patagonian Andes (Argentina). J Hydrol 2012a;444–445:134–45.

Worni R, Huggel C, Stoffel M, Pulgarín B. Challenges of modeling current very large lahars at Nevado del Huila Volcano, Colombia. Bull Volcanol 2012b;74:309–24.

Yamada T, Sharma CK. Glacier lakes and outburst floods in the Nepal Himalaya. IAHS-AISH Publ 1993;218:319–30.